

## DIELECTRIC RESONATOR FILTERS

Because microwave filtering is an important function required to keep a number of different systems in working order, the specifications of a filter are varied. We can, however, try to classify some of them as presented in Table 1. The constraints are electrical, mechanical, thermal, and commercial.

The objective in this article is to show the advantages of the dielectric resonator (DR) technique to satisfy some of these functions, along with its disadvantages, in comparison with some other well-known solutions.

DRs are suitable for bandpass filtering. DR filters are classified as three-dimensional (3D) devices, in opposition to two-dimensional (2D) planar ones.

The main advantages of 2D solutions are their relative bycompact dimensions, their easier integration in circuit or module environment, and their well-known design and manufacturing procedures. They are, however, limited in their applications to the processing of low power, sizable relative bandwidth signal, in relation to the poor unloaded quality factor of localized microwave elements or planar resonators. Some solutions are proposed to restrict losses, such as applying superconductors or active-element techniques, but they remain inadequate to replace 3D devices, in particular for high-power requirements.

In the class of 3D devices, designers have first chosen waveguides or metallic empty cavities to satisfy their very narrow bandwidth filtering requirements. However, since the mid-1980s, high-dielectric-constant materials, having low loss tangent and good thermal stability, have become available. The DR solution has been preferred for a number of applications, in particular spatial ones. This technique allows us to reduce significantly the cavities and waveguide device sizes, for equivalent electrical and increased thermal performances. Some average ratios can be given for dual-mode resonators (DR compared with cavity):

- 1 : 4 in volume
- 1 : 2 in mass

Moreover, the DR shape and the mode in which it is excited can be chosen to give a response to particular requirements, as we will see later in this article. A number of DR shapes and filter topologies have, however, been proposed. Our work here is limited to the presentation of the most popular ones.

In this article, we present some characteristic parameters of DR filters, which are generally introduced during the synthesis procedure. These definitions are helpful in explaining the choices of filter designers, in particular the DR shapes and arrangements in multipole devices.

In Section 1, the class of devices loaded by cylindrical DRs is investigated. This is a common shape for the DR. It can be excited on a symmetric mode ( $TE_{0n}$  or  $TM_{0m}$ ) or on a first hybrid mode ( $HEM_{11}$ ). Different DR arrangements in the filter are presented and discussed.

For particular applications in microwave filtering, we can fit the DR shape or the DR mode. For high-power applications, it is important to put the high-dielectric-constant

material in contact with a metallic enclosure, to improve the thermal dissipation. DRs of a quarter-cut cylinder, a cylindrical rod, or a dielectric plate shielded in a metallic cavity are investigated. Solutions are also given to optimize the isolation of the filter response on the frequency axis, or to apply DR to the millimeter wave filtering. These particular applications are included in Section 2.

Approaches developed to design DR filters are discussed in Section 4. A four-pole DR filter synthesis is proposed as an example.

## ELECTRICAL CHARACTERISTIC PARAMETERS OF A DR FILTER

Applying conventional methods, the design of microwave filters starts with the selection of an ideal transfer function that fulfills the electrical objectives of the specifications. The synthesis of this ideal transfer function leads to an equivalent lumped-element circuit. This circuit is characterized by a coupling matrix that depends on the lumped-element values. A number of studies have been devoted to this task (1, 2). Different circuit topologies can be chosen. However, for the DR filters presented in this article, the equivalent circuit is close to the one presented in Fig. 1 (canonical symmetric design). Nevertheless, if another solution is chosen, the same characteristic parameters may have to be computed.

From the circuit presented Fig. 1, we define the following:

- The central frequency of the filter:

$$f_0 = \frac{1}{2\pi\sqrt{LC}} \quad (1)$$

- The unloaded quality factor of each resonator:

$$Q_0 = \frac{L\omega_0}{R}, \quad \omega_0 = 2\pi f_0 \quad (2)$$

- The input and output coupling coefficients. In the electrical scheme, the coupling levels between the excitation access ( $P_1$  and  $P_2$ ) and the first and last resonators (1 and  $n$ ) are characterized, respectively, by the ratios  $1/n_1$  and  $1/n_2$ . It is however generally preferred to define external quality factors  $Q_{ei}$  (1) at port  $i$ , ( $i \in \{1, 2\}$ ), by

$$Q_{ei} = \frac{2\pi L f_0}{R_{ei}} \text{ with} \quad (3)$$

$$R_{ei} = R_0 n_i^2 \quad (4)$$

as the external loading resistance at port  $P_i$ . Coupling coefficients  $\alpha_i$  are also defined at port  $i$  by

$$\alpha_i = \frac{Q_0}{Q_{ei}} \quad (5)$$

- The coupling coefficient between resonators. The resonators are intercoupled, longitudinally and crosswise, in the general case. We define a coupling coefficient  $K_{ij}$  between resonators  $i$  and  $j$  by

$$K_{ij} = \frac{M_{ij}}{L} \quad (6)$$

Table 1. Microwave Filter Specifications

Electrical	Mechanical	Thermal	Commercial
Central frequency	Mass and volume	Temperature range of use	Components and materials costs
Passband width	Vibration resistance	Maximum dissipated power	Machining cost
Passband ripple	Machining tolerances	Sensitivity of electrical response to temperature variations	Design cost
Out-of-band selectivity and rejection	Manufacturing difficulties		Delay for design and realization of filter
Response isolation			
Insertion losses			
SWR			
Group delay			
Power capabilities			

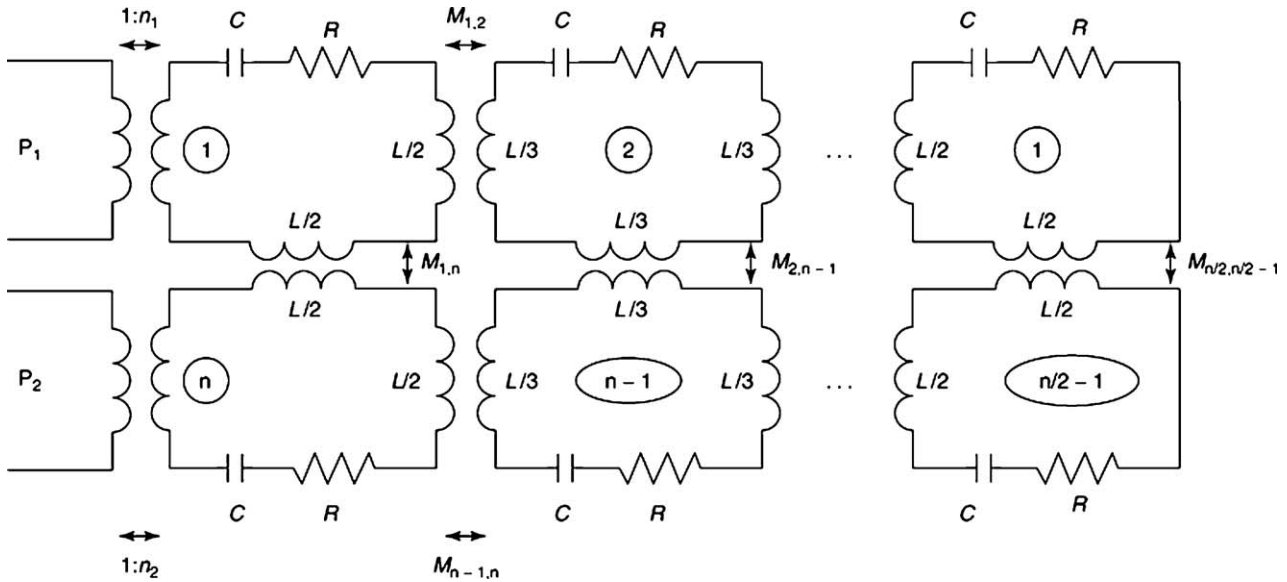


Figure 1. Equivalent circuit of a symmetric  $n$ -pole filter.

The crosswise coupling coefficients (except  $K_{n/2,n/2-1}$ ) may cancel to obtain conventional Butterworth or Chebyshev responses. Some of them are different from zero and can be negative for elliptic bandpass function realizations, including transmission zeros in the out-of-band part of the transmission response.

These parameters help the designer perform the third synthesis step, the computation of the device dimensions. The topology of the filter, in particular the DR arrangement, is easily directly deduced from the equivalent-circuit one, which, in fact, justifies this approach. In Section 3, we explain how the dimensions of the filter are computed from knowledge of the parameters  $f_0$ ,  $M_{ij}$ , and  $Q_{ei}$ .

### FILTERS COMPOSED OF CYLINDRICAL DRS

Cylindrical DRs are more often used to realize multipole filters. We discuss this class of solutions here. The DR is generally shielded in a metallic box, to avoid radiation losses. It can then be excited on transverse electric

$TE_{0n}$  modes, transverse magnetic  $TM_{0m}$  modes, or hybrid  $HEM_{nm}$  modes. The natures of the transmission lines or waveguides used to couple the filter, the nature of the DRs arrangement in the device, and the nature of the electrical, mechanical, and thermal characteristics of the filter depend on the choice of the DR mode. Table 2 compares the performance levels of the  $TE_{01}$ ,  $TM_{01}$ , and  $HEM_{11}$  modes. The dimensions are optimized to obtain a resonant frequency equal to 4 GHz. We notice that the DR acting on the  $TE_{01}$  mode is the less bulky one. Even if the electrical performances are comparable, the  $TM_{01}$  mode is more radiative in the cavity, which increases the metallic losses on the enclosure. The  $HEM_{11}$  mode is in fact very interesting for reduction of filter size. The filter performance of each particular TE, TM, or hybrid mode is discussed below.

### Monomode Filter

The DRs are excited on the symmetric  $TM_{01}$  or  $TE_{01}$  modes. An  $n$ -pole “monomode” filter is then composed of  $n$  DRs. The dimensions of each DR and of the metallic enclosure are generally chosen to optimize, at the filter center frequency,

Table 2. Comparison between  $TE_{01}$ ,  $TM_{01}$ ,  $HEM_{11}$ , and  $DR^{1001}$  Mode Performance Levels

	$f_0$ (GHz)	$Q_0$	$D_{RD}$ (mm)	$H_{RD}$ (mm)	$D_C$ (mm)	$H_c$ (mm)
$TE_{01}$	4	8600	14	5.5	28	19.5
$TM_{01}$	4	7500	28	8.3	52	56
$HEM_{11}$	4	9600	19.3	6	40	20

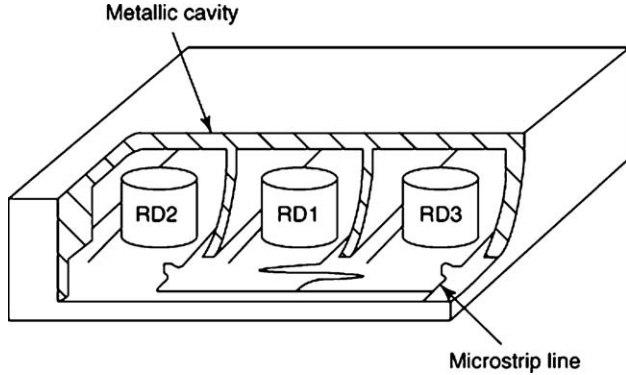


**Figure 3.** DR lines excited on a  $TE_{01}$  mode through microstrip lines.

the dielectric and metallic losses and the device sizes, as well as to avoid spurious responses around the filter bandpass.

Different topologies of the  $TE_{01}$  mode, have been reported in the literature. The DRs can be placed side by side on the same plane. To obtain good isolation on this mode, the ratio between diameter and height of each DR is generally chosen to be 2. Then the radial radiation of each DR is small and the DRs can be coupled directly; a metallic iris does not have to be placed systematically between the DRs to limit the filter size.

Two examples of realization are presented in Figs. 2,3. Different techniques can be employed to couple the filter. Propagative rectangular waveguides can be connected to both ends of a waveguide section above cutoff, which contains the DR. The  $TE_{01}$  mode of the DRs is excited if their axis are positioned along the wide dimension of the monomode waveguide (Fig. 2). The distances between the first (and respectively last) DR and the junctions between the waveguide sections enable us to tune the level of the input (respectively output) coupling coefficient. This technique is suitable for high-power applications.

To improve the integration of the filter in its environment, we must couple the first and last DRs to microstrip lines (Fig. 3). Nevertheless, the metallic losses of such a structure increases, as the DR must be placed near the metallic strip and ground plane to obtain the required coupling levels. The evolution of the coupling coefficient as a function of the distance between the line and the DR is given in Ref. 3.

Dielectric resonators might also be coupled through coaxial probes (4) or loops (5). Particular attention to the positioning of the excitation systems around the DR enable us to obtain a good isolation of the bandpass response on the frequency axis.

From the devices shown in Figs. 2a and 2b (4–6), we obtain narrow-bandpass Chebyshev or Butterworth re-

sponses. Stopband filters can also be realized easily using these DR coupling techniques, coupling the DR to a propagative waveguide or a transmission line (7).

Coupling the DRs side by side enables us to maintain them easily, such as on a dielectric substrate, whose material is chosen to improve the temperature stability of the filter. Moreover, some tuning elements can be integrated around the DRs; some metallic or dielectric screws are generally placed along the DRs axis to tune the filter resonant frequency, as well as between the DRs to adjust the coupling coefficients.

On the  $TE_{01}$ ,  $TM_{01}$ , and  $TM_{02}$  modes, DRs have also been mounted axially on a cylindrical dielectric rod. To obtain an elliptic response on these symmetric modes, in the same device we can combine axial and side-by-side mounting configurations. A two-stage device is constructed. The transversal coupling  $M_{ij}$  can then be achieved, as it has been done for empty metallic cavities. A negative coupling is obtained by setting some upper and lower cavity axis; the resulting transmission zeros placed around the passband response increase the filter selectivity (8).

Different techniques, including those mentioned previously, have been developed for the mounting of DRs in their enclosure; for instance, the DRs can be glued on a dielectric support. This technique may, however, be critical because of the generation of parasitic gaps between the glued materials and the poor glue loss tangent. A mounting based on a differential dilatation phenomenon between each DR and its environment is more suitable for obtaining high electrical performance. The capability of the filter to withstand vibration is fundamental for space applications. Some test measurements are given, for example, in Ref. 9.

### Dual-Mode Filters

Dual-mode filters (10) are now widely used because they offer equivalent electrical performance levels, smaller size, and less mass than do classical fundamental TE or TM-mode filters. A metallic screw, or another perturbation is placed around the DR to break the rotational symmetry. Then, on the first or second hybrid mode, the two polarizations sections are imposed, and their frequencies differ in relation to the perturbation dimension. Figure 4 presents a two-pole dual-mode filter, composed of only one DR. Two monomode DRs would be coupled to obtain the same electrical response. The DR is excited through coaxial probes. Two tuning screws are generally added in the excitation probe axis to tune the central resonant frequency.

The coupling screw is placed at an angle of  $45^\circ$  from the excitation axis. In this case, the symmetry of the structure suffices to fix the direction of the two polarizations. The electromagnetic environment of each mode differs; thus the resonant frequencies  $f_1$  and  $f_2$  of the two polarizations differ. The power combining is constructive between  $f_1$  and

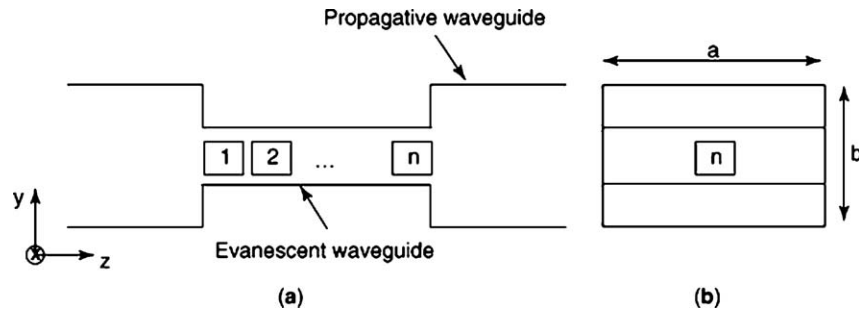


**Figure 2.** DRs excited on a  $TE_{01}$  mode through rectangular waveguides.

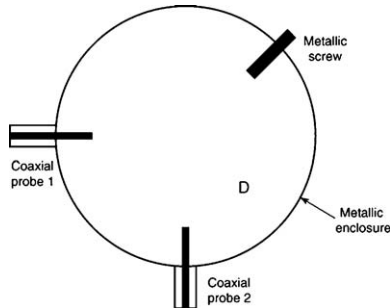


**Figure 4.** Dual-mode DR excited by two coaxial probes.

$f_2$  at the output access, which explains the bandpass response obtained from this device. Some transmission zeros are also observed, due to the combination of opposite phases between the two polarizations, and between these phases and a higher-order mode of the DR (11).

For  $n$ -pole elliptic realization, with  $n > 2$  and  $n$  as an odd number, we need to couple parallel modes in adjacent DRs (longitudinal coupling) and to avoid extra coupling between orthogonal modes of different DRs. Three screws are placed around each DR as shown in Fig. 4, and adjacent DRs are generally iris-coupled. Two orthogonal rectangular apertures machined in a metallic plate enable us to impose the required coupling level between each set of parallel polarizations. To obtain a negative sign on some crosswise coupling coefficients, the different screws are not positioned at the same angle with the excitations in the different cavities. This technique is well known for metallic cavity realizations (12). An example of four-pole topology is presented in Fig. 5, where the DRs are coupled to input–output coaxial probes.

The excitation can also take the form of rectangular waveguides, coupled to the input–output cavities through rectangular irises, for power applications. These irises are then generally placed in a plane perpendicular to the DR axis.

Adjacent DRs can also be coupled directly, rather than iris coupled (13). Then realizations of small coupling levels may require large separation between adjacent DRs, and may consequently require significant sizes. However, the introduction of evanescent waveguide sections between DRs enable us to reduce the device dimensions (14). The drawbacks of this method are the filter spurious characteristics and the dependent coupling level between the mode sets of adjacent DRs. In the same way as monomode real-

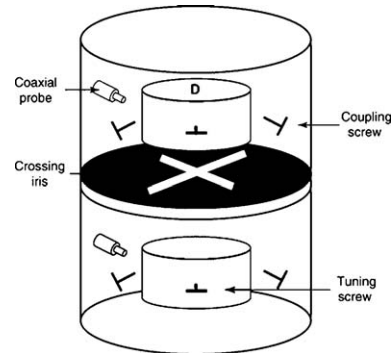


**Figure 5.** Example of four-pole dual-mode DR filter.

izations, dual-mode DRs can be mounted in a planar relationship to one another. Each DR is again enclosed in a metallic cavity. The DR intercouplings are controlled independently by a metallic iris that contains two rectangular noncrossing apertures placed in an appropriate manner (15). This solution is interesting for its flexibility in the arrangement of the DR cavities.

More than two modes have also been coupled in the same DR cavity, to conserve weight and size in comparison with the previous solutions. The two polarizations of the  $HEM_{11}$  modes and the  $TM_{01}$  mode have been simultaneously excited in a planar DR-mounted cavity. Two of these three-pole modules have been coupled through an iris composed of two separate T-shaped apertures (16).

## PARTICULAR APPLICATIONS OF DRS IN MICROWAVE FILTERING

### DR for High-Power Applications

The dual-mode devices we have presented above are interesting for their high electrical performance levels and limited sizes. But even if the filter dissipated power is small, the resulting thermal dissipation remains critical for certain applications, such as space applications, because the thermal conductivity of most dielectric material is poor.

A solution consists of positioning the high permittivity resonators in contact with the metallic enclosure, to improve the thermal dissipation efficiency, and then to improve the power-handling capability of the filter.

We can first take advantage of the electromagnetic field symmetry of a cylindrical DR. It can be divided into two or more parts, without modifying the resonant frequency

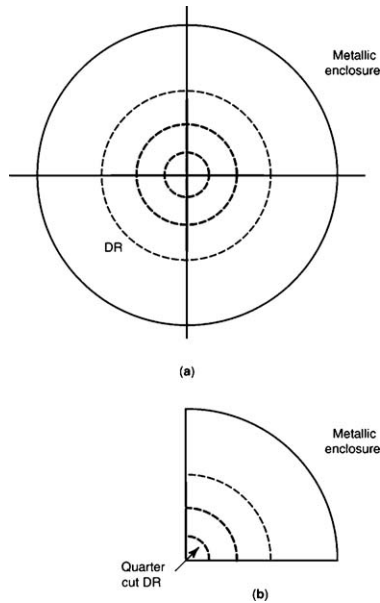


**Figure 6.** Equivalent cylindrical (a) and quarter-cut (b) DRs excited on a  $TE_{01}$  mode (— electric field lines).

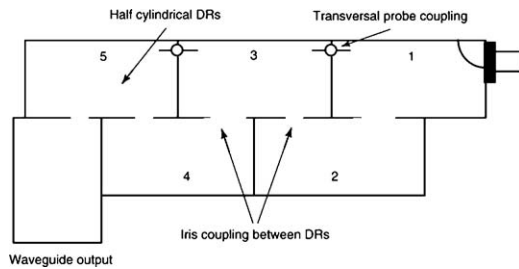


**Figure 7.** Five-pole elliptic filter using the split-DR technique.

and field repartition of some modes, if the physical metallic walls are placed in planes in which electrical wall conditions are naturally verified (17, 18). In this way a cylindrical DR excited on a  $TE_{01}$  mode can be split, for example, into four parts. If each of the cut planes are in contact with a metallic wall (Fig. 6), all quarter-cut DRs will resonate at the same frequency.

The improvement of the power-handling capability is not the sole purpose of this technique. A number of cylindrical DR modes do not satisfy the electrical wall condition in the planes where they are imposed on the quarter-cut DR. They are then suppressed in the “image” DR. Hence the out-of-band rejection performances of the filter is improved, suppressing spurious responses.

This technique also provides very compact structures, reducing the size not only of the DR but also of the metallic enclosure. This is an important advantage, particularly for 900-MHz–3-GHz applications. Nevertheless, the metallic losses on the metallic plane in contact with the DR increase dramatically, resulting in a poor unloaded quality factor  $Q_0$  of the DR. We can note, however, that the image resonator might be preferred to coaxial dielectric field resonators, considering the sizes and losses at the same frequency. Figure 7 presents a possible arrangement of the DRs to realize an elliptic five-pole function (17).

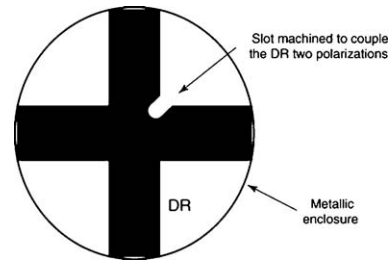


**Figure 8.** TM dual-mode resonator.

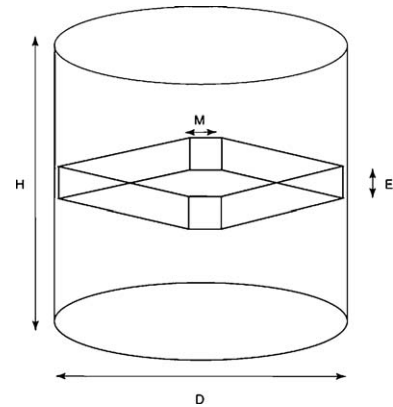


**Figure 9.** High-permittivity dielectric plate resonator technique.

Different techniques have been proposed to increase the unloaded quality factor of the split DR. TM dual-mode DRs have been developed for use in the L and C frequency bands for mobile communication applications. A cross is formed as shown in Fig. 8, by two parallelepipedic DRs excited on a  $TM_{01}$  mode (19). The tuning element required to couple the two degenerated modes is not a metallic screw, but a perturbation directly machined near the center of the cross. An unloaded quality factor equal to 9000 has been obtained at 1.9 GHz, for a dielectric loss tangent equal to  $5 \times 10^{-5}$  (20). A high-permittivity dielectric plate has also been placed in a metallic enclosure to provide a good compromise between the unloaded quality factor level and the thermal dissipation capability (21). The corners of a thin parallelepipedic plate have been cut to provide a good contact between the resonator and a cylindrical metallic cavity (Fig. 9).

The dimensions are optimized to limit the metallic and dielectric losses on the first TE mode that has degenerated. It has been shown that the electrical performance of this resonator is not far from that of the cylindrical dual-mode one, and this solution is more suitable for power applications. Metallic screws are generally placed around the dielectric plate to couple the first TE polarizations. Slots are then machined in the plate, both to couple these polarizations and to optimize the out-of-band rejection of the filter. Superimposed cavities are coupled through metallic cross irises. The topology of an eight-pole autocorrected quasielliptic filter is presented in Fig. 10. The transmission and reflection responses, along with the group delay of the filter, are presented in Fig. 11.

Some other studies have been performed to optimize the DR shape to increase the unloaded quality factor of the resonators, in particular by choosing adequate forms of the

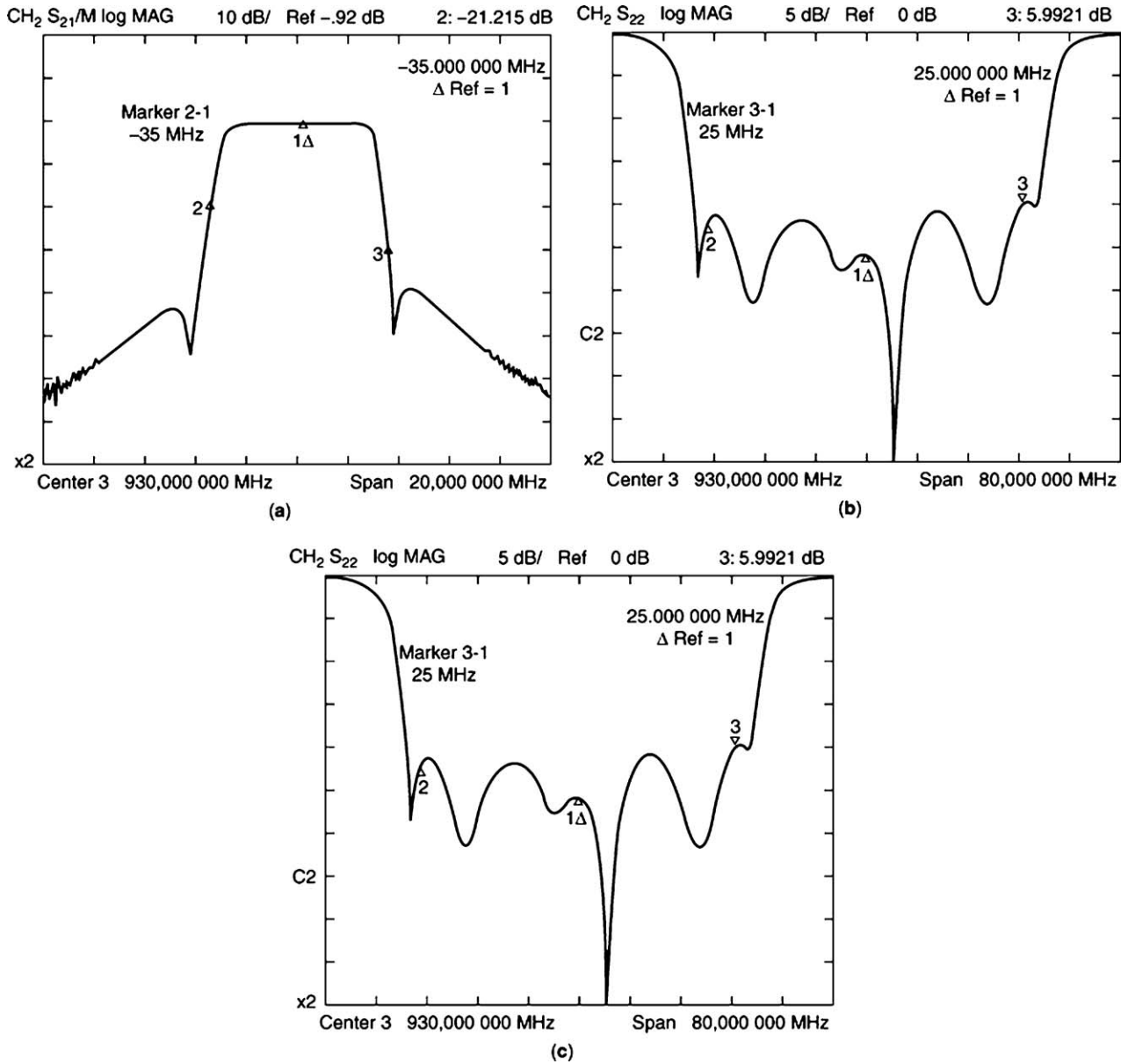


**Figure 11.** (a,b) Transmission and reflection coefficient variations as a function of the frequency; (c) group delay variation in filter passband.

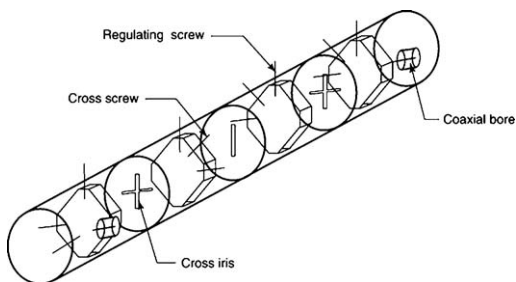


**Figure 10.** Dielectric plate eight-pole connected elliptic filter.

DR dielectric support in contact with the metallic enclosure (22).

### Filter Configurations for Optimization of Out-of-Band Rejection

Conventional DR filters have relative poor stopband rejection performance, due to the excitation of higher-order mode resonances. A lowpass filter, placed at the output of the bandpass DR filter, might solve this problem, but the bulk and the electrical performance of the cascaded filter suffer from this solution. Different filter configurations have, however, been proposed to increase the out-of-band rejection.

We have already underlined that the quarter-cut DR, or the  $TM_{01}$  DR, which are of interest for power applications, are also efficient techniques for elimination of some of the spurious responses.

Coupling structures have been designed to suppress the excitation of some modes. A single-mode  $TE_{01}$  filter realization is, for example, presented in Ref. 23. The diameter: height ratio of the DR is generally chosen to optimize the mode isolation. A hole can be machined in the cylindrical DR, along its axis (24, 25), and the DR shape can be matched (26) to increase this isolation. A more sophisticated solution consists of mixing DRs excited on different modes in a same filter. To obtain part of the ring DR isolation, and part of the compactness of dual-mode devices,  $TE_{01}$  ring DRs and a  $HEM_{11}$  dual-mode DR have been coupled to realize six-pole elliptic filters, combining four DRs. DRs can be mounted axially (27) or side by side (28) in their metallic enclosures. As an example, the center frequency of the realized filter is equal to 1.23 GHz; its passband is 20 MHz, and the out-of-band rejection is better than  $-40$  dB in the 1–1.9 GHz frequency band (27).

### DR for High-Frequency Applications

When the frequency increases, the dimensions of cylindrical DRs excited on the first  $TE_{01}$ ,  $TM_{01}$ , and  $HEM_{11}$  modes become too small. The limit of conventional DR applications can be set around 20 GHz. To solve the manufacturing problem, spherical DRs have been proposed. But the critical mechanical stability of the devices, along with the spurious modes around the bandpass limits their applications.

We can, however, use cylindrical DRs on whispering gallery modes (29). For important azimuthal variation number, the DR can be used easily up to 100 GHz. Moreover, the field is very effectively stored in with the DR, and the unloaded quality factor, which thus depends only on the material loss tangent, is important. Examples of filter realizations are given in Ref. (30).

## THEORETICAL DESIGN OF MICROWAVE DR FILTERS

### Introduction

DRs are used for the realization of narrowband filters up to 0.01% relative bandwidth. The electrical responses of such devices are then very sensitive to their geometric and physical characteristics, and particular attention must be paid to their design.

The purpose of the theoretical design can be not only to optimize the filter performances but also to reduce the cost of the product. If the design is not efficient, the time required for the tuning can be important; different devices are manufactured, and even in the phase when the dimensions are known, an experimenter must spend time and effort to tune each filter.

However, DR structures are difficult to analyze, because their geometries are very complex. We have seen that the filter topologies are diverse; DRs can be intercoupled or coupled through a metallic iris; they may be excited by coaxial probes, metallic waveguides, and microstrip lines;

their shapes are not systematically cylindrical; and they can be maintained in their metallic enclosures through a wide variety of systems. Moreover, the structures are very compact, and if we can define different segments in its composition, strong couplings are generated between the DRs through high-order modes. Thus the classical approach that is applied in the circuit software, namely, the segmentation method, is not efficient here; we cannot characterize each segment independently from the others, and we cannot connect the different contributions to obtain the device response.

Analytical-approach models were initially developed to assist designers. These methods are described in Ref. 31. Since the late 1980s, rigorous analyses have been performed, first on some parts of the DR filter. Examples include application of modal methods (32, 33), the finite-element method (34), or the method of lines (35) to characterize axisymmetric dielectric-loaded metallic cavities, computing the resonant frequencies of these devices. Some other studies have been performed on the design of three-dimensional resonator, which is nonsymmetrical in structure. The resonant frequency of a DR shielded in a parallelepipedic enclosure has been computed applying the modal method (36) and the finite-element method (37, 38). From these computations we can easily deduce the coupling coefficient between two DRs for symmetric structures. The coupling coefficient between a DR and a waveguide or a transmission line has been computed by applying the finite-element method (39, 40). Now, with the evolution of computer capabilities, a number of research teams are interested in the electromagnetic optimization of DR devices applying numerical simulation. A number of articles deal with the rigorous design of multipole filters. In this section we will describe a solution for the rigorous design of a multipole DR filter using the finite-element method (40).

### Method for Optimized Design of a DR Filter

The procedure generally applied to determine the geometric dimensions of a multipole filter is deduced from the lumped-element synthesis presented in Section 1. To explain this approach, we have chosen here to design a dual-mode four-pole DR filter because this design groups together some problems found in a large variety of DR filter topologies. In the dual-mode DR presented in Section 1, the metallic screws are replaced by slots directly machined in the DR. The four-pole filter, shown in Fig. 12, consists of a metallic cavity, two input/output coaxial probes, and two slotted DRs coupled through metallic cross irises. Because the experimental filter will not be tuned, the synthesis procedure has to be performed rigorously. To compute the filter dimensions that satisfy given electrical characteristics, we develop the approach presented in Fig. 13.

In the first stage, an equivalent lumped-element circuit is synthesized from the ideal transfer function. The synthesis leads to a coupling matrix that characterizes the ideal equivalent circuit. This objective coupling matrix gives all the information about the ideal electrical characteristic parameters of the filter.

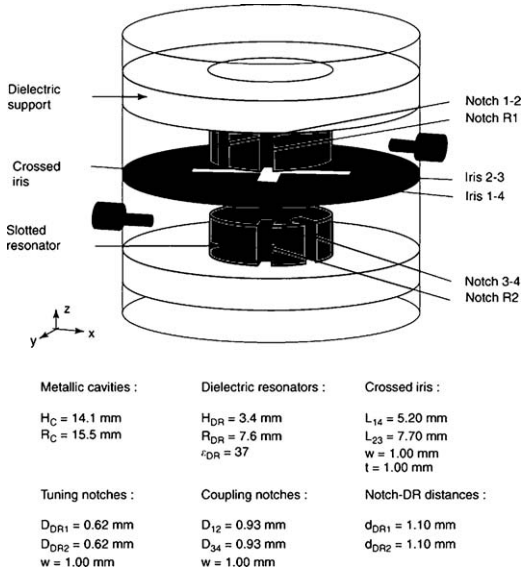


Figure 12. Four-pole slotted DR filter.

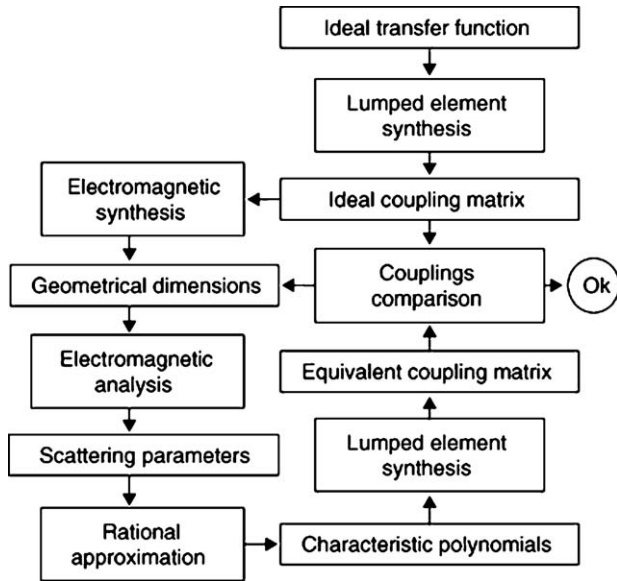


Figure 13. Design method of multipole filter.

Applying the 3D finite-element method (40), we can then compute the initial dimensions of the structure with respect to the previous electrical parameters. An electromagnetic synthesis allows us to determine the following:

1. The DR and metallic cavity dimensions required to satisfy the center frequency  $f$  value.
2. The probe depth penetration, computed to obtain the required input/output coupling coefficient levels.
3. The dimension of the cross iris to obtain the required coupling coefficient between the parallel polarizations of the two DRs. The theoretical synthesis method is generally interrupted here for classical applications. Screws are then placed around the filter to couple the polarizations and to account for the resonant frequencies of the filter. Then a set of irises are

manufactured, and each experimental device has to be tuned. Choosing the slotted DR solution, we can continue with the synthesis computations.

4. The coupling notch dimensions, which impose the coupling coefficient between the two polarizations of each DR.
5. The dimensions of a second notch, which are introduced to compensate for the influence of the probes and the iris on the resonant frequency of the excited polarization.

Then, all the dimensions of the device presented in Fig. 12 are known, but only approximately because of the segmentation approach applied in these initial steps, which does not account for the indirect dependence between the different elements.

In the third stage, an electromagnetic optimization loop is performed applying the following procedure:

1. The 3D finite-element method is applied in order to compute the scattering parameters between the access ports of the whole structure.
2. The scattering parameters are approximated as rational functions in the frequency domain.
3. From the approximated rational functions, an equivalent circuit, namely, a coupling matrix, of the simulated filter is synthesized.
4. By comparing the extracted coupling matrix and the ideal one, the filter dimensions are corrected according to the dimension sensitivities from the electromagnetic synthesis.

The loop is performed as long as the electrical objective is not attained.

This procedure is detailed in Refs. 40 and 41. The ideal transfer function and the electromagnetic response at the end of the optimization are compared in Fig. 14. We can note the good convergence of the electromagnetic model response with a return loss of  $>30 \text{ dB}$  in the passband. In Ref. 40, the filter is designed with a slightly different filtering pattern. The electromagnetic response along with the experimental results are presented in Fig. 15. The filter is realized and measured without tuning elements. The difference between the computed and measured center frequencies is less than 0.2%, and the difference between the bandwidths is less than 5%. The theoretical and experimental standing-wave ratios are in good agreement.

## CONCLUSION

DRs are currently placed in a number of devices, especially in microwave filters. The topologies of these filters are diverse, and they are a function of the system in which they are placed. Their main applications are found in the treatment of power signals and very narrow bandwidth filtering.

In this article, we have described different topologies proposed in recent years (as of 2004). A number of research teams are still working to increase the performance of DR filters, and to widen their domain of applications. Some of



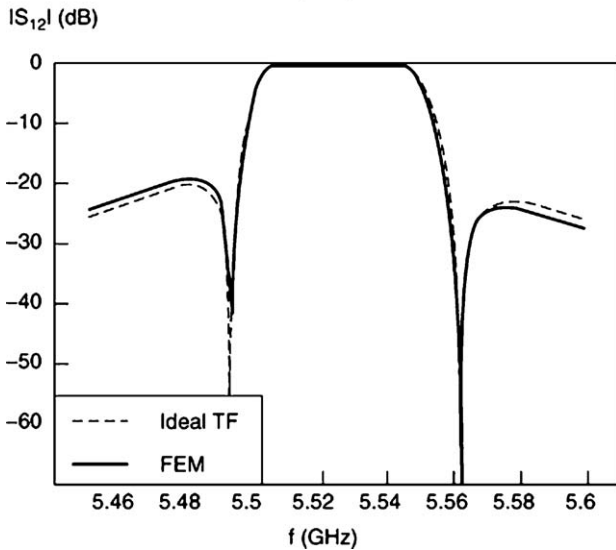
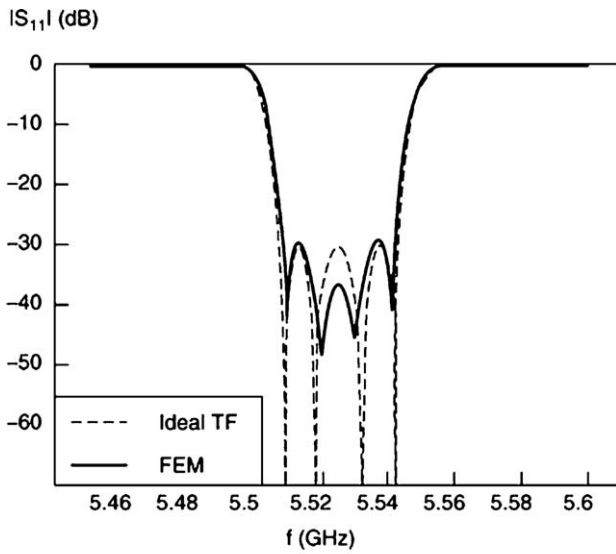


Figure 14. Comparison of ideal and electromagnetic results.

the topics under consideration are the following:

- The realization of filters in the millimeter wavelength band
- The work performed to decrease the volume and weight of DR devices
- The realization of DR filters without mechanical tuning for mass production
- The design of reconfigurable DR filters for multifrequency band applications
- The development of advanced synthesis techniques for simplified design of DR filters (42), for example, with a minimum number of elements

## BIBLIOGRAPHY

1. G. Matthaei, L. Young, and E. M. T. Jones, *Microwave Filters, Impedance Matching and Coupling Structures*, Artech House, Dedham, MA, 1963.
2. A. E. Atia, A. E. Williams, and M. W. Newcomb, Narrowband multiple coupled cavity synthesis, *IEEE Trans. Circ. Syst. CAS-21*(5): 649–655 (Sept. 1974).
3. D. Chaimbault, S. Verdeyme, and P. Guillon, Rigorous design of the coupling between a dielectric resonator and a microstrip line, Proc. 24th European Microwave Conf. (EMC), Cannes, Sept. 5–8, 1994.
4. Y. Kobayashi and M. Minegishi, A low loss band pass filter using electrically coupled high  $Q$   $TM_{01d}$  dielectric rod resonators, *IEEE Trans. Microwave Theory Tech.* **36**(12): 1727–1732 (Dec. 1988).
5. T. Nishikawa *et al.*, *Microwave Bandpass Filter Provided with Dielectric Resonators*, U.S. Patent 4,143,344 (March 6, 1979).
6. S. B. Cohn, Microwave band pass filters containing high  $Q$  dielectric resonators, *IEEE Trans. Microwave Theory Tech.* **16**: 218–277 (April 1968).
7. C. V. Ren, Waveguides band stop filter utilizing  $Ba_2 Ti_9 O_{20}$  resonators, Proc. 1978 Int. Microwave Symp. June 1978, p. 227.
8. A. E. Atia and A. E. Williams, General  $TE_{011}$  mode waveguide band pass filters, *IEEE Trans. Microwave Theory Tech.* **24**(10): 640 (Oct. 1976).

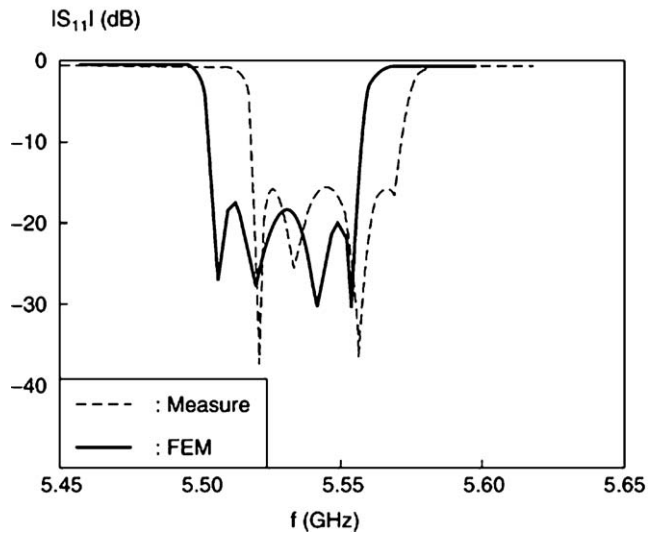
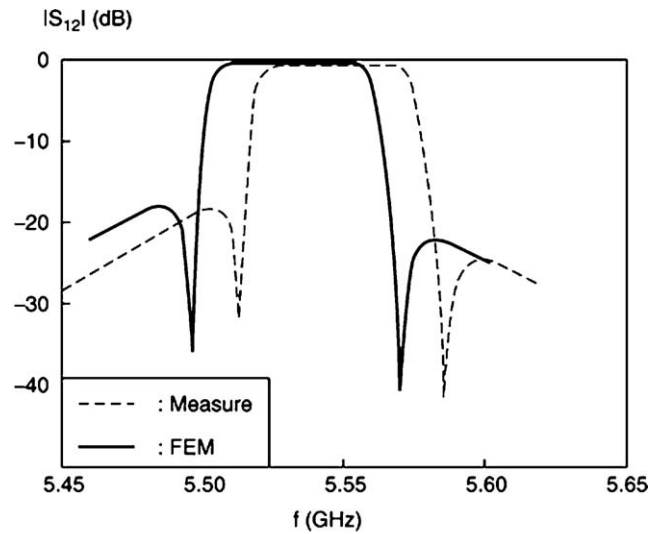


Figure 15. Comparison of theoretical and measured results.

9. S. Vigneron, B. Theron, V. Madrangeas, F. Tounsi, and P. Guillon, Dielectric resonators filters for space applications, Proc. ESA-ESTEC Workshop on Microwave Filters for Space Applications, June 1990, pp. 71–80.
10. S. J. Fiedziusko, Dual mode dielectric resonator loaded cavity filters, *IEEE Trans. Microwave Theory Tech.* **30**(9): 1311–1316(Sept. 1982).
11. D. Baillargeat, S. Verdeyme, and P. Guillon, Symmetrical quasi elliptic two pole dielectric resonator filter, *Electron. Lett.* **31**(11): 893–895(May 25, 1995).
12. A. E. Atia and A. E. Williams, New types of waveguide band pass filters satellite transponders, *Comsat Tech. Rev.* **1**(1): 21–43( 1971).
13. K. A. Zaki, C. Chen, and A. E. Atia, Canonical and longitudinal dual mode dielectric resonator without iris, *IEEE Trans. Microwave Theory Tech.* **35**(12): 1130–1135(Dec. 1987.)
14. S. C. Chen and K. A. Zaki, A novel coupling method for dual mode dielectric resonators and waveguide filters, *IEEE Trans. Microwave Theory Tech.* **38**(12): 1885–1892(Dec. 1990).
15. W. C. Tang, D. Siu, B. C. Beggs, and J. Sferazza, *Planar Dual Mode Cavity Filters including Dielectric Resonators*, U.S. Patent 4,652,843, March 24, 1987.
16. W. C. Tang, D. Siu, B.C. Beggs, and J. Sferazza, *Triple Mode Dielectric Loaded Band Pass Filter*, U.S. Patent 4,675,630(June 23, 1987).
17. T. Nishikawa, K. Wakino, K. Tsunoda, and Y. Ishikawa, Dielectric high power band pass filter using quarter cut  $TE_{018}$  image resonator for cellular base structures, *IEEE MTT-S Digest*, 1987, pp. 133–136.
18. R. J. Cameron, W. C. Tang, and L. M. Kudsia, Advances in dielectric loaded filters and multiplexers for communications satellites, Proc. ESA/ESTEC Workshop on Microwave Filters for Space Applications, Noordwijk June 1990.
19. K. Wakino, T. Nishikawa, and Y. Ishikawa, Miniaturization technologies of dielectric resonator filters for mobile communications, Proc. MTT Workshop on Filters and Multiplexers for Mobile Communications, June 17, 1993.
20. Y. Ishikawa, J. Hattori, S. Abe, E. Kobayashi, and T. Nishiyawa, 1.9 GHz compact low loss dielectric diplexer designer by dual mode waveguide transmission line method, Proc. 24th European Microwave Conf. (EMC), Sept. 1994, Vol. 2, pp. 1179–1184.
21. S. Moraud, S. Verdeyme, P. Guillon, Y. Latouche, S. Vigneron, and B. Theron, A new dielectric loaded cavity for high power microwave filtering, *IEEE MTT-S Digest*, 1996, Vol.2, pp. 615–618.
22. S. Gendraud, S. Moraud, S. Verdeyme, P. Guillon, S. Vigneron, and B. Theron, New miniaturized dielectric loaded cavity microwave resonators, Proc. 25th European Microwave Conf. (EMC), Bologne, Sept. 1995, pp. 691–695.
23. R. V. Snyder, Dielectric resonator filter with wide stop bands, *IEEE Trans. Microwave Theory Tech.* **40**: 2100–2102(Nov. 1992).
24. Y. Kobayashi and M. Miura, Optimum design of shielded dielectric rod and ring resonators for obtaining the best mode separation, *IEEE MTT-S Digest*, 1984, Vol.1, pp. 184–186.
25. S. W. Chen and K. A. Zaki, Dielectric ring resonators loaded in waveguide and on substrate, *IEEE Trans. Microwave Theory Tech.* **39**: 2069–2076(Dec. 1991).
26. R. M. Mansour, Dual mode dielectric resonator filter with improved spurious performance, *IEEE MTT-S Digest*, 1993, pp. 443–446.
27. J. F. Liang, K. A. Zaki, and A. E. Atia, Mixed modes dielectric resonator loaded cavity filters, *IEEE MTT-S Digest*, 1994, pp. 731–734.
28. C. Wang, H. W. Yao, and K. A. Zaki, Mixed modes cylindrical planar dielectric resonator filters with rectangular enclosure, *IEEE MTT-S Digest*, 1995, Vol.2, pp. 501–504.
29. X. H. Jiao, P. Guillon, L. A. Bermudez, and P. Auxemery, Whispering gallery modes of dielectric structures: Application to millimeter wave bandstop filters, *IEEE Trans. Microwave Theory Tech.* **35**(12): 1169–1175(Dec. 1987).
30. D. Cros, F. Nigon, P. Besnier, M. Aubourg, and P. Guillon, Whispering gallery dielectric resonator filters, *IEEE MTT-S Digest*, 1996, Vol.2, pp. 603–606.
31. D. Kajfez and P. Guillon, *Dielectric Resonators*, Artech House, Dedham, MA, 1986.
32. W. K. Hui and I. Wolff, A multicomposite, multilayered cylindrical dielectric resonator for applications in MMIC's. *IEEE Trans. Microwave Theory Tech.* **2**(3): 415–423(March 1994).
33. K. A. Zaki, Electromagnetic simulation of dielectric resonator devices using mode matching technique, Proc. MTT-S Workshop WFFA, Dielectric Resonators in Microwave Active and Passive Circuits, San Francisco, 1996.
34. P. S. Kooi *et al.*, Finite element analysis of the shielded cylindrical dielectric resonators, *IEE Proc.* **132**(Part H)(1): 7–16(Feb. 1995).
35. D. Kremer and R. Pregla, The method of lines for the hybrid analysis of multilayered dielectric resonators, *IEEE MTT-S Digest*, Orlando, 1995, Vol.2, pp. 491–494.
36. X. P. Liang and K. A. Zaki, Modeling of cylindrical dielectric resonators in rectangular waveguides and cavities, *IEEE Trans. Microwave Theory Tech.* **41**(12): 2174–2181(Dec. 1993).
37. R. Ferrari and G. Maille, Three dimensional finite element method for solving electromagnetic problems, *Electron. Lett.* **14**(15): 467–468(July 1978).
38. S. Verdeyme, M. Aubourg, and P. Guillon, Three dimensional finite element method applied to dielectric resonators devices, <bookTitle>IEEE MTT-S</book>, Los Angeles, 1989.
39. J. P. Cousty, S. Verdeyme, M. Aubourg, and P. Guillon, Finite element for microwave device simulations: Applications to microwave DRs filters, *IEEE Trans. Microwave Theory Tech.* **40**(5): 925–932(May 1992).
40. D. Baillargeat, S. Verdeyme, P. Guillon, and M. Guglielmi, New dual mode coupling using slotted dielectric resonator, *Microwave Opt. Technol. Lett.* (Jan. 1993).
41. S. Bila, D. Baillargeat, S. Verdeyme, M. Aubourg, P. Guillon, F. Seyfert, J. Grimm, L. Baratchart, C. Zanchi, and J. Sombrin, Direct electromagnetic optimization of microwave filters, *IEEE Microwave Mag.* **2**(1): 46–51(March 2001).
42. S. Bila, D. Baillargeat, S. Verdeyme, F. Seyfert, L. Baratchart, C. Zanchi, and J. Sombrin, Simplified design of microwave filters with a symmetric transfer functions, Pro. 33rd European Microwave Conf. (EuMW 03), Munich, Germany, Oct. 2003.

S. BILA  
D. BAILLARGEAT  
S. VERDEYME  
P. GUILLON  
IRCOM, Limoges, France